Why Does Symmetry Cause Deadlocks ?

Jaskaran Grover*   Changliu Liu**   Katia Sycara***

The Robotics Institute, Carnegie Mellon University, USA
(email: {*jaskarag,**cliu6,***sycara}@andrew.cmu.edu)

Abstract: Collision avoidance for multirobot systems has been studied thoroughly. Recently, control barrier functions (CBFs) have been proposed to mediate between collision avoidance and goal achievement for multiple robots. However, it has been noted that reactive controllers (such as CBFs) are prone to *deadlock*, an equilibrium that causes the robots to stall before reaching their goals. In this paper, we formally analyze two and three robot systems and discover circumstances under which CBFs cause deadlocks using duality theory. For the two robot system, we consider mutually heterogeneous robots (such as one more vigorous or closer to its goal than the other) and prove that this heterogeneity does not help in preventing deadlock. We then consider three robots, and conclude from these two scenarios that the geometric symmetry resulting from robots' initial positions and goals constrains CBFs to generate velocities that render deadlock stable. Thus, conferring skewness to the system can help evade deadlock.

Keywords: Mobile robots, Multiagent systems, Autonomous robotic systems, Robotics technology, Model predictive and optimization-based control

1. INTRODUCTION

Multirobot systems have been explored for many tasks, such as environmental exploration, search and rescue and sensor coverage (Cortes et al. (2004); Burgard et al. (2005); Kantor et al. (2003)). Running local controllers on individual robots results in global behaviors (Olfati-Saber et al. (2007)), that allows a team of robots to accomplish tasks not easily achievable by a single robot. Generally, these local controllers combine a task-based control responsible for a primary objective and a collision avoidance controller. However, such a hand-engineered combination can prevent satisfaction of the original task. Therefore, we focus on a formal analysis of the performance-safety trade-off that may result from augmenting a task-based controller with collision avoidance constraints. One example of such a mechanism is control barrier function (CBF) based quadratic programs (QPs) (Ames et al. (2017)). In the context of multirobot control (Borrmann et al. (2015)), CBF-QPs mediate between performance and safety in a rigorous way. They perform minimum modification to the task-based control in a way that generates a velocity/acceleration, which by virtue of design, prevents collisions of the ego robot with its neighbors. While provably correct, these local approaches can exhibit a lack of look-ahead, which causes robots to be trapped in *deadlocks* as noted in (Petti and Fraichard (2005); O'Donnell (1989)).

Deadlock occurs when robots reach a state where conflict becomes inevitable, *i.e.* a control favoring goal stabilization will violate safety. In the context of mobile robots, Yamaguchi (1999) identified the presence of deadlocks in a cooperative scenario using mobile robot troops. To our knowledge, Jager and Nebel were the first to propose algorithms for deadlock resolution for multiple robots. Their strategy for collision avoidance modifies planned paths by inserting idle times and resolves deadlocks by asking the planners to plan an alternative trajectory until deadlock is resolved. Li et al. (2005) proposed coordination graphs to resolve deadlocks in robots navigating in corridors. Rodríguez-Seda et al. (2016) added perturbations to their controllers for avoiding deadlock. Wang et al. (2017) proposed consistent perturbations to evade deadlock.

Our work, on the other hand, analytically deduces why deadlocks occur by investigating robots' dynamics w.r.t. initial conditions, goal positions and controller gains using duality theory. Our proofs for incidence of deadlock help us to arrive at conclusions without simulations, making the analysis general. We highlight with examples that *it is the geometric symmetry in the robots' initial positions and goals that constrains CBF-QPs to generate controls in directions that render deadlock stable.* Additionally, our approach for analyzing CBF-QPs using duality can be applied to any optimization based reactive control-synthesis methods (Wei and Liu (2019)) and guide the design of algorithms for synthesis of bottleneck-free controllers.

The outline of this paper is as follows: in Section (2), we review technical definitions for CBF-QPs for multirobot control. In Section (3), we give a formal definition of deadlock and demonstrate that KKT conditions provide a valuable tool to explicitly analyze solutions to CBF-QPs. In Section (4), we focus on two robots with heterogeneous parameters and collinear initial conditions and goals, and formally prove that this system always falls in deadlock. In Section (5), we extend this analysis to three robots and prove that this system also falls in deadlock. Finally, we conclude with discussion and directions for future work.

2. AVOIDANCE CONTROL WITH CBFs: REVIEW

In this section, we review the background on CBF based QPs, which we will use for synthesizing controllers for each robot in the multirobot system. (See Wang et al. (2017) for a comprehensive treatment). Assume we have N robots, where each robot follows single-integrator dynamics

$$\dot{\boldsymbol{p}}_i = \boldsymbol{u}_i \qquad (1)$$

Here $\boldsymbol{p}_i = (x_i, y_i) \in \mathbb{R}^2$ is the position of robot i and $\boldsymbol{u}_i \in \mathbb{R}^2$ is its velocity (*i.e.* control input) and $i \in \{1, 2, \cdots, N\}$. The problem of goal stabilization with collision-avoidance requires that each robot i must reach a goal position $\boldsymbol{p}_{d_i}$ while avoiding collisions with every other robot j, $\forall j \in \{1, 2, \cdots, N\} \backslash i$. Assume that there is a user-prescribed proportional controller $\hat{\boldsymbol{u}}_i(\boldsymbol{p}_i) = -k_{p_i}(\boldsymbol{p}_i - \boldsymbol{p}_{d_i})$ that generates movement towards goal. Here k_{p_i} is the controller gain for robot i. Although this controller by itself ensures stabilization of each robot to its goal, there is no guarantee that the resulting trajectories of the robots will be mutually collision free. We formulate a pairwise safety function that maps the joint state space of robots i and j to a real-valued safety index *i.e.* $h : \mathbb{R}^2 \times \mathbb{R}^2 \longrightarrow \mathbb{R}$:

$$h_{ij} = \left\| \Delta \boldsymbol{p}_{ij} \right\|^2 - D_s^2 \qquad (2)$$

Robots i and j are considered to be collision-free if their positions $(\boldsymbol{p}_i, \boldsymbol{p}_j)$ are such that $h_{ij}(\boldsymbol{p}_i, \boldsymbol{p}_j) \geq 0$ (*i.e.* atleast D_s distance apart). Assuming that initial positions are collision-free *i.e.* $h_{ij}(\boldsymbol{p}_i(0), \boldsymbol{p}_j(0)) \geq 0$, we would like to synthesize controls $\boldsymbol{u}_i, \boldsymbol{u}_j$ that ensure their future positions are also collision-free *i.e.* $h_{ij}(\boldsymbol{p}_i(t), \boldsymbol{p}_j(t)) \geq 0$, $\forall t > 0$. This can be achieved by ensuring that (Ames et al. (2017))

$$\frac{dh_{ij}}{dt} \geq -\gamma h_{ij}, \qquad (3)$$

where $\gamma > 0$. Using (2) in (3), we get

$$-\Delta \boldsymbol{p}_{ij}^T \Delta \boldsymbol{u}_{ij} \leq q_{ij}, \text{ where} \qquad (4)$$

$$q_{ij} = \frac{\gamma}{2}(\left\| \Delta \boldsymbol{p}_{ij} \right\|^2 - D_s^2) \qquad (5)$$

This constraint is distributed on robots i and j as:

$$-\Delta \boldsymbol{p}_{ij}^T \boldsymbol{u}_i \leq \frac{1}{2} q_{ij} \text{ and } \Delta \boldsymbol{p}_{ij}^T \boldsymbol{u}_j \leq \frac{1}{2} q_{ij} \qquad (6)$$

Therefore, any $\boldsymbol{u}_i$ and $\boldsymbol{u}_j$ that satisfy (6) are guaranteed to ensure collision free trajectories for robots i and j in the multirobot system. Note that these constraints are linear in $\boldsymbol{u}_i$ and $\boldsymbol{u}_j$ for a given state $(\boldsymbol{p}_i, \boldsymbol{p}_j)$. Therefore, the feasible set of controls is convex. Since robot i wants to avoid collisions with $N-1$ robots, there are $N-1$ collision avoidance constraints. To mediate between safety and goal stabilization objective, a QP is posed that computes a controller closest to the prescribed control $\hat{\boldsymbol{u}}_i(\boldsymbol{p}_i)$ and satisfies the $N-1$ constraints, as shown:

$$\begin{aligned} \boldsymbol{u}_i^* = \underset{\boldsymbol{u}_i}{\arg\min} \quad & \| \boldsymbol{u}_i - \hat{\boldsymbol{u}}_i(\boldsymbol{p}_i) \|^2 \\ \text{subject to} \quad & \boldsymbol{a}_{ij}^T \boldsymbol{u}_i \leq b_{ij} \; j \in \{1, 2, \cdots, N\} \backslash i \end{aligned} \qquad (7)$$

where using (6), we define

$$\boldsymbol{a}_{ij} := -\Delta \boldsymbol{p}_{ij} \;, \quad b_{ij} := \frac{1}{2} q_{ij} = \frac{\gamma}{4}(\left\| \Delta \boldsymbol{p}_{ij} \right\|^2 - D_s^2) \qquad (8)$$

Each robot i locally solves this QP to determine its $\boldsymbol{u}_i^*$, which ensures collision avoidance of robot i with $N-1$ robots while encouraging motion towards goal.

3. ANALYSIS USING KKT CONDITIONS

We reviewed the problem formulation of multirobot collision avoidance and goal stabilization using CBF based QPs. We will demonstrate that controls generated using this framework can result in deadlocks. First, we give a formal definition of deadlock by adapting from Wang

et al. (2017) (where it is defined for double-integrator dynamics):

Definition 1. *A robot i is said to be in deadlock if $\boldsymbol{u}_i^* = 0$ and $\hat{\boldsymbol{u}}_i \neq 0 \iff \boldsymbol{p}_i \neq \boldsymbol{p}_{d_i}$*

This definition states that for a robot to be in deadlock, the output from the QP based controller *i.e.* the velocity of the robot should be zero, even though the prescribed controller reports non-zero velocity because the robot is not at its intended goal. To characterize situations in which deadlock occurs, we need to analytically investigate solutions of (7) $\forall i \in \{1, 2, \cdots, N\}$ because these solutions govern the instantaneous dynamics of the robots. We will use this instantaneous analysis to make deductions about the robots' motion in the long term.

To this end, KKT conditions provide a valuable tool to investigate solutions to optimization problems such as the QP in (7). They are necessary and sufficient for a global optimum of this QP. The Lagrange dual function is

$$L(\boldsymbol{u}_i, \boldsymbol{\mu}_i) = \| \boldsymbol{u}_i - \hat{\boldsymbol{u}}_i \|_2^2 + \sum_{j \in \{1, 2, \cdots, N\} \backslash i} \mu_{ij}(\boldsymbol{a}_{ij}^T \boldsymbol{u}_i - b_{ij})$$

Let $(\boldsymbol{u}_i^*, \boldsymbol{\mu}_i^*)$ be the optimal primal-dual solution to (7). The KKT conditions are (Boyd and Vandenberghe (2004))

(1) Stationarity: $\nabla_{\boldsymbol{u}_i} L(\boldsymbol{u}_i, \boldsymbol{\mu}_i)|_{(\boldsymbol{u}_i^*, \boldsymbol{\mu}_i^*)} = 0$

$$\implies \boldsymbol{u}_i^* = \hat{\boldsymbol{u}}_i - \frac{1}{2} \sum_{j \in \{1, 2, \cdots, N\} \backslash i} \mu_{ij}^* \boldsymbol{a}_{ij}^T. \qquad (9)$$

(2) Primal Feasibility

$$\boldsymbol{a}_{ij}^T \boldsymbol{u}_i^* \leq b_{ij} \; \forall j \in \{1, 2, \cdots, N\} \backslash i \qquad (10)$$

(3) Dual Feasibility

$$\mu_{ij}^* \geq 0 \; \forall j \in \{1, 2, \cdots, N\} \backslash i \qquad (11)$$

(4) Complementary Slackness

$$\mu_{ij}^* \cdot (\boldsymbol{a}_{ij}^T \boldsymbol{u}_i^* - b_{ij}) = 0 \; \forall j \in \{1, 2, \cdots, N\} \backslash i \qquad (12)$$

We define the set of active and inactive constraints as

$$\mathcal{A}(\boldsymbol{u}_i^*) = \{j \in \{1, 2, \cdots, N\} \backslash i \mid \boldsymbol{a}_{ij}^T \boldsymbol{u}_i^* = b_{ij}\} \qquad (13)$$

$$\mathcal{IA}(\boldsymbol{u}_i^*) = \{j \in \{1, 2, \cdots, N\} \backslash i \mid \boldsymbol{a}_{ij}^T \boldsymbol{u}_i^* < b_{ij}\} \qquad (14)$$

Using complementary slackness from (12), we deduce

$$\mu_{ij}^* = 0 \; \forall j \in \mathcal{IA}(\boldsymbol{u}_i^*) \qquad (15)$$

Therefore, we can restrict the summation in (9) only to the set of active constraints *i.e.*

$$\boldsymbol{u}^* = \hat{\boldsymbol{u}}_i - \frac{1}{2} \sum_{j \in \mathcal{A}(\boldsymbol{u}_i^*)} \mu_{ij}^* \boldsymbol{a}_{ij}^T \qquad (16)$$

We will exploit this representation of controls to explore scenarios in which deadlock occurs. We conducted many simulations where multiple robots were tasked to reach some goals using (7). We observed that the incidence of deadlock depends on the initial positions of robots and their goals, the gains k_{p_i} and the distances of initial positions to goals (D_{G_i}). Therefore, next, we formally analyze the dependence of deadlock on these parameters.

4. TWO ROBOT DEADLOCK

Firstly, we consider two robots positioned on the line connecting their goals at $t = 0$ as shown in Fig. (1). Each robot must reach its respective goal while avoiding collisions with
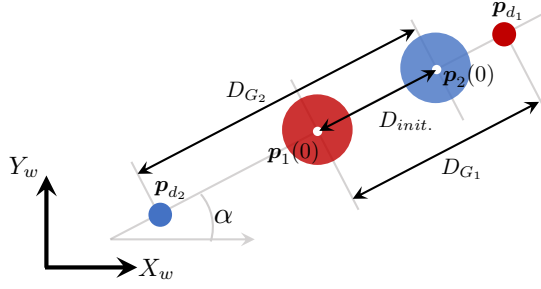
Fig. 1. Geometric configuration of two robots and their goals. Notice that everything is collinear along $\hat{\boldsymbol{e}}_\alpha$.

the other robot. We will demonstrate that even if the prescribed control of one robot is more aggressive than the other, (7) will still result in deadlock because of the collinearity of initial conditions and goals. Let $\boldsymbol{p}_i(t) \in \mathbb{R}^2$ denote the position of robot $i \in \{1, 2\}$ at time t. At $t = 0$,

$$\boldsymbol{p}_1(0) = (x_0, y_0)$$
$$\boldsymbol{p}_2(0) = \boldsymbol{p}_1(0) + D_{init}\hat{\boldsymbol{e}}_\alpha \qquad (17)$$

where $\hat{\boldsymbol{e}}_\alpha$ is a unit vector oriented at α relative to X_w axis and $D_{init} \in \mathbb{R}^+$ is the initial distance between the robots (see Fig. (1)). The desired goal positions are

$$\boldsymbol{p}_{d_1} = \boldsymbol{p}_1(0) + D_{G_1}\hat{\boldsymbol{e}}_\alpha$$
$$\boldsymbol{p}_{d_2} = \boldsymbol{p}_2(0) - D_{G_2}\hat{\boldsymbol{e}}_\alpha \qquad (18)$$

Here D_{G_i} is the distance of robot i from its goal $\boldsymbol{p}_{d_i}$ at $t = 0$. We assume that $D_{G_1}, D_{G_2} > D_{init}$ to encourage situations where deadlock occurs. We now formally state the deadlock incidence result as follows

Theorem 1. *Given the initial positions of robots as in (17) and desired goals as in (18), the controls generated by the QP in (7) will cause the robots to fall in deadlock $\forall D_{G_1}, D_{G_2} > D_{init}$ and $\forall k_{p_1}, k_{p_2} \in \mathbb{R}^+$*

We first give the general sketch of the proof to convey the overall idea. Recall from (16) that the control input on robot i at every time step, depends on whether the collision avoidance constraint is active or inactive at $\boldsymbol{u}_i = \boldsymbol{u}_i^*$. Therefore, to begin with, we analyze the controls returned by (7) at $t = 0$. In **Lemma 2**, we show that if the initial distance between the robots is greater than a certain critical distance, then the collision avoidance constraints of both robots are inactive, and as a result $\boldsymbol{u}_i^*(0) = \hat{\boldsymbol{u}}_i(0) \forall i$. We then extend this analysis to future time $t > 0$ and show that there exist three sequential phases of motion which are dependent on which robot's constraint is active/inactive. These phases are:

(1) Phase 1 corresponds to the duration in which the collision avoidance constraints of both robots are inactive. We show that this phase culminates in a finite time and the robots move closer to each other during this phase (**Lemma 3**) .

(2) Next, phase 2 begins where one robot's constraint becomes active while the other's is still inactive. This is due to the heterogeneity $k_{p_1} \neq k_{p_2}$ and $D_{G_1} \neq D_{G_2}$. We show that phase 2 also culminates and the robots move closer to each other (**Lemma 4**).

(3) Finally, Phase 3 begins where both constraints are active. We show that the distance between robots converges to the safety margin D_s and the robots stop

moving (**Lemma 5**), while they are still away from their goals, thus proving they have fallen in *deadlock*.

For the special case of two robots, the control for robot i can be written by adapting (16),

$$\boldsymbol{u}_i^* = \hat{\boldsymbol{u}}_i - \frac{1}{2}\mu_{ij}\boldsymbol{a}_{ij} \qquad (19)$$

where $j \neq i$ and $i \in \{1, 2\}$. Recall that $\hat{\boldsymbol{u}}_i$ is a user prescribed proportional controller for robot i

$$\hat{\boldsymbol{u}}_i = -k_{p_i}(\boldsymbol{p}_i - \boldsymbol{p}_{d_i}) \qquad (20)$$

In Section (3), we showed that the value of Lagrange multiplier μ_{ij} depends on whether the collision avoidance constraint $\boldsymbol{a}_{ij}^T\boldsymbol{u}_i \leq b_{ij}$ is active/inactive at $\boldsymbol{u}_i = \boldsymbol{u}_i^*$ Thus, we will have two flags for the two robots:

$$f_{ij}(\boldsymbol{u}_i) = \boldsymbol{a}_{ij}^T\boldsymbol{u}_i - b_i, \qquad (21)$$

$\forall i \in \{1, 2\}$ and $j \neq i$. This flag checks if control $\boldsymbol{u}_i$ prevents robot i from colliding with robot j. Note that if $f_{ij}(\hat{\boldsymbol{u}}_i) < 0$, then $\mu_{ij} = 0$ (from complementary slackness (12)). Therefore, from (19) it follows that $\boldsymbol{u}_i^* = \hat{\boldsymbol{u}}_i$.

Remark 1: $f_{ij}(\hat{\boldsymbol{u}}_i) < 0$ for $j \neq i$ implies that $\hat{\boldsymbol{u}}_i$ is a feasible collision-avoiding controller for robot i w.r.t. j, and since the cost in (7) penalizes deviation from $\hat{\boldsymbol{u}}_i$, the optimum is attained with zero penalty at $\boldsymbol{u}_i^* = \hat{\boldsymbol{u}}_i$ itself.

Next, we give conditions under which the collision avoidance constraints are active/inactive. Define critical distances for robot i as (to be derived in **Lemma 2**)

$$\beta_+^i = \frac{2D_{G_i}k_{p_i}}{\gamma} + \sqrt{\left(\frac{2D_{G_i}k_{p_i}}{\gamma}\right)^2 + D_s^2} \qquad (22)$$

$\forall i \in \{1, 2\}$. We now show that if the initial distance between the robots is greater than robot i's critical distance, then robot i has inactive constraint at $t = 0$.

Lemma 2. *If at $t = 0$, $D_{init.} > \beta_+^1$, then $\boldsymbol{u}_1^*(0) = \hat{\boldsymbol{u}}_1(0)$. Likewise, if $D_{init.} > \beta_+^2$, then $\boldsymbol{u}_2^*(0) = \hat{\boldsymbol{u}}_2(0)$*

Proof. To determine the control returned by the optimization for robot one at $t = 0$, we compute the value of the flag $f_{12}(\hat{\boldsymbol{u}}_1(0))$. Based on the initial positions and goals from (17),(18), we have

$$\begin{aligned}f_{12}(\hat{\boldsymbol{u}}_1(0)) &= \boldsymbol{a}_{12}^T(0)\hat{\boldsymbol{u}}_1(0) - b_{12}(0) \\ &= k_{p_1}(\boldsymbol{p}_1(0) - \boldsymbol{p}_2(0))^T(\boldsymbol{p}_1(0) - \boldsymbol{p}_{d_1}) \\ &\quad - \frac{\gamma}{4}(D_{init.}^2 - D_s^2) \\ &= -\frac{\gamma}{4}D_{init}^2 + D_{G_1}k_{p_1}D_{init} + \frac{\gamma}{4}D_s^2 \qquad (23)\end{aligned}$$

We define $g_{12}(D_{init.}) \coloneqq f_{12}(\hat{\boldsymbol{u}}_1(0))$ to emphasize dependence of this flag on $D_{init.}$, the initial distance between the robots. Note that (23) is a quadratic polynomial in D_{init} that opens downward and has two zeros at

$$\beta_\pm^1 = \frac{2D_{G_1}k_{p_1}}{\gamma} \pm \sqrt{\left(\frac{2D_{G_1}k_{p_1}}{\gamma}\right)^2 + D_s^2} \qquad (24)$$

where the subscript of β indicates the sign of β. Now, since the graph of $g_{12}(D_{init})$ is a downward facing parabola, we know that $g_{12}(D_{init}) < 0 \ \forall \ D_{init} \in (-\infty, \beta_-^1) \cup (\beta_+^1, \infty) \implies g_{12}(D_{init}) < 0 \ \forall \ D_{init} \in (\beta_+^1, \infty)$. We call β_+^1 to be the critical distance for robot 1 (as defined in (22)). If at $t = 0$, the distance between the robots

is such that $D_{init} > \beta_+^1$, then at $t = 0$, $g_{12}(D_{init.}) < 0 \iff f_{12}(\hat{\boldsymbol{u}}_1(0)) < 0 \implies \boldsymbol{u}_1^*(0) = \hat{\boldsymbol{u}}_1(0)$. This follows from Remark 1. Similarly, we can compute $g_{21}(D_{init.}) := f_{21}(\hat{\boldsymbol{u}}_2(0))$ which has roots at $\beta_{\pm}^2$. Hence, if at $t = 0$, $D_{init} > \beta_+^2$, then $\boldsymbol{u}_2^*(0) = \hat{\boldsymbol{u}}_2(0)$. ∎

Intuitively, this result states that if robot i is sufficiently away from robot $j \neq i$ (specifically more than β_+^i away), then robot i can simply use it's prescribed controller $\hat{\boldsymbol{u}}_i$ at $t = 0$ and not worry about collisions at least until the next time. Note from (22) that each robot has a unique critical distance which solely depends on that robot's k_{p_i}, D_{G_i}, which is due to the assumed heterogeneity.

Assumption 1. *WLOG assume that $D_{init.} > \beta_+^1 > \beta_+^2$*

From assumption (1), and the result of Lemma 2, it follows that the collision avoidance constraints of both robots are inactive at $t = 0$. Thus, $\boldsymbol{u}_i^*(0) = \hat{\boldsymbol{u}}_i(0)$ for $i = \{1, 2\}$. If we give these velocities to robots for a small time Δt, the distance between the robots and the critical distance will change. So at the next time, we will compare the updated distance between robots with the updated critical distances to decide whether $\boldsymbol{u}_i^*(\Delta t) = \hat{\boldsymbol{u}}_i(\Delta t)$ and so on. It suffices to assume that these constraints remain inactive for finite time, which is precisely the duration of phase 1.

4.1 Phase 1

We consider phase 1 to be the period in which the collision avoidance constraints of both robots are inactive *i.e.*

$$f_{12}(\hat{\boldsymbol{u}}_1(t)) = \boldsymbol{a}_{12}^T(t)\hat{\boldsymbol{u}}_1(t) - b_{12}(t) < 0 \qquad (25)$$

$$f_{21}(\hat{\boldsymbol{u}}_2(t)) = \boldsymbol{a}_{21}^T(t)\hat{\boldsymbol{u}}_2(t) - b_{21}(t) < 0 \qquad (26)$$

Thus, we define the duration of phase 1 to be

$$t_1 := \sup_{t>0}\{t | f_{12}(\hat{\boldsymbol{u}}_1(t)) < 0, f_{21}(\hat{\boldsymbol{u}}_2(t)) < 0\} \qquad (27)$$

Lemma 3. *∃ a finite time t_1 as described in Def. (27), until which the collision avoidance constraints of both robots are simultaneously inactive.*

Proof. Let us assume that until time t_1, the collision avoidance constraints of both robots are inactive. Thus, both robots simply use their prescribed controls $\hat{\boldsymbol{u}}_i(t)$ until t_1^-. Therefore, the dynamics of the robots are

$$\dot{\boldsymbol{p}}_i = \hat{\boldsymbol{u}}_i = -k_{p_i}(\boldsymbol{p}_i - \boldsymbol{p}_{d_i}) \qquad (28)$$

(28) can be integrated using Eqs. (17) and (18) to give

$$\boldsymbol{p}_1(t) = \boldsymbol{p}_{d_1} - D_{G_1}e^{-k_{p_1}t}\hat{\boldsymbol{e}}_\alpha$$
$$\boldsymbol{p}_2(t) = \boldsymbol{p}_{d_2} + D_{G_2}e^{-k_{p_2}t}\hat{\boldsymbol{e}}_\alpha \qquad (29)$$

We can compute the relative positions as

$$\Delta\boldsymbol{p}_{21}(t) = (D_{G_1}e^{-k_{p_1}t} + D_{G_2}e^{-k_{p_2}t} - K)\hat{\boldsymbol{e}}_\alpha$$
$$= D(t)\hat{\boldsymbol{e}}_\alpha \qquad (30)$$

where $K := D_{G_1} + D_{G_2} - D_{init}$ and $D(t) := (D_{G_1}e^{-k_{p_1}t} + D_{G_2}e^{-k_{p_2}t}) - K$. Thus, the distance between the robots is

$$\left\|\Delta\boldsymbol{p}_{d_{21}}(t)\right\| = |D(t)| \qquad (31)$$

Additionally, the controls as a function of time are

$$\hat{\boldsymbol{u}}_1(t) = -k_{p_1}(\boldsymbol{p}_1(t) - \boldsymbol{p}_{d_1}) = +k_{p_1}D_{G_1}e^{-k_{p_1}t}\hat{\boldsymbol{e}}_\alpha \quad (32)$$

$$\hat{\boldsymbol{u}}_2(t) = -k_{p_2}(\boldsymbol{p}_2(t) - \boldsymbol{p}_{d_2}) = -k_{p_2}D_{G_2}e^{-k_{p_2}t}\hat{\boldsymbol{e}}_\alpha \quad (33)$$

Thus, the flag for robot 1 is (25)

$$f_{12}(\hat{\boldsymbol{u}}_1(t)) = \boldsymbol{a}_{12}^T(t)\hat{\boldsymbol{u}}_1(t) - b_{12}(t)$$
$$= -\frac{\gamma}{4}D^2(t) + k_{p_1}D_{G_1}e^{-k_{p_1}t}D(t) + \frac{\gamma}{4}D_s^2$$

which is a downwards facing parabola in $D(t)$. Thus, $f_{12}(\hat{\boldsymbol{u}}_1(t)) < 0$ for $D(t) > \beta_+^1(t)$ where

$$\beta_+^1(t) = \frac{2D_{G_1}k_{p_1}e^{-k_{p_1}t}}{\gamma} + \sqrt{\left(\frac{2D_{G_1}k_{p_1}e^{-k_{p_1}t}}{\gamma}\right)^2 + D_s^2} \tag{34}$$

and likewise we can define $\beta_+^2(t)$ for robot two by replacing k_{p_1}, D_{G_1} with k_{p_2}, D_{G_2} in (34). Note that $D(t)$, $\beta_+^1(t)$ and $\beta_+^2(t)$ are monotonically decreasing with time. Additionally, recall from (17) that $D(0) = D_{init.}$ and from from Assumption 1 that $D_{init.} > \beta_+^1$. However, while $D(t)$ converges to $-(D_{G_1} + D_{G_2} - D_{init}) < 0$, $\beta_+^1(t), \beta_+^2(t)$ converge to $D_s > 0$. Therefore, there exists a time t_a at which $D(t_a) = \beta_+^1(t_a) \implies f_{12}(\hat{\boldsymbol{u}}_1(t_a)) = 0$ and a time t_b at which $D(t_b) = \beta_+^2(t_b) \implies f_{21}(\hat{\boldsymbol{u}}_2(t_b)) = 0$. We assume WLOG that $\beta_+^1(t_1) > \beta_+^2(t_1) \implies t_a < t_b$ and hence we define:

$$t_1 := \min\{t_a, t_b\} = t_a \tag{35}$$

t_a is the time at which the collision avoidance constraint of robot one becomes active *i.e.* $\boldsymbol{a}_{12}^T(t_a)\boldsymbol{u}_1^*(t_a) = b_{12}(t_a)$ while the collision avoidance constraint of robot two is still inactive *i.e.* $\boldsymbol{a}_{21}^T(t_a)\hat{\boldsymbol{u}}_2(t_a) < b_{21}(t_a)$. Thus t_a is the time in Def. 27, *i.e.* the maximum time until which both robots' constraints are inactive. See Fig. (2) for an illustration of phase 1 which ends at $t = t_1$ when $D(t) = \beta_+^1(t)$. Finally, $D(t)$ is monotonically decreasing $\forall t$ (30) and $D(0) = D_{init.} > 0$, $D(t_1) = \beta_+^1(t_1) > 0$, therefore, $D(t) > 0$ $\forall t \in [0, t_1)$. From (31) that the distance between the robots is $\|\Delta\boldsymbol{p}_{21}(t)\| := |D(t)| = D(t) \; \forall t \in [0, t_1)$. Therefore, $\|\Delta\boldsymbol{p}_{21}(t)\|$ is also monotonically *decreasing* until t_1. ∎

Thus, phase 1 ends at time t_1 when the constraint of robot one switches from inactive to active, while that of robot two is still inactive. This marks the beginning of phase 2.

4.2 Phase 2

Consistent with the definition of t_1 (27), we define the duration of phase 2 to be the time until which the constraint of robot two remains inactive *i.e.*

$$t_2 := \sup_{t>t_1}\{t | f_{21}(\hat{\boldsymbol{u}}_2(t)) < 0\} \tag{36}$$

Recall from phase 1 that $f_{21}(\hat{\boldsymbol{u}}_2(t)) < 0$ as long as $D(t) > \beta_+^2(t)$. However, after t_1, $D(t)$ no longer follows (30) because of the change in dynamics of robot one after t_1. Therefore, we will compute new dynamics for $D(t)$ and a time t_2 when $D(t) = \beta_+^2(t)$.

Lemma 4. *∃ a finite time t_2 as in Def. (36), until which the constraint of robot two stays inactive.*
Proof. Let us assume that there is a time t_2 until which the collision avoidance constraint of robot two remains inactive. Therefore, the dynamics of robot two are governed by the prescribed input. Thus,

$$\dot{\boldsymbol{p}}_2 = \hat{\boldsymbol{u}}_2 = -k_{p_2}(\boldsymbol{p}_2 - \boldsymbol{p}_{d_2})$$
$$\implies \boldsymbol{p}_2(t) = \boldsymbol{p}_{d_2} + D_{G_2}e^{-k_{p_2}t}\hat{\boldsymbol{e}}_\alpha \tag{37}$$

On the other hand, the control input to robot one is

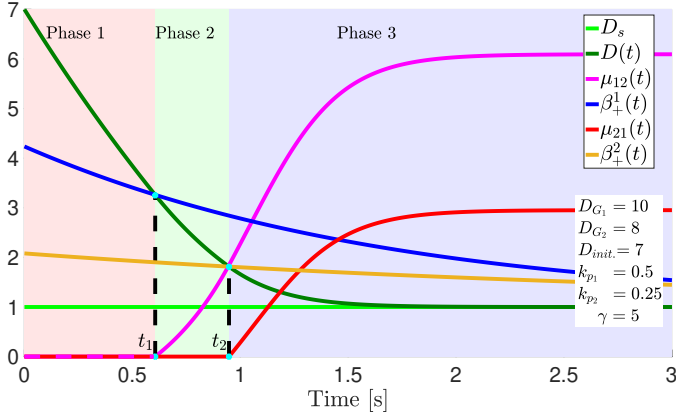$$\boldsymbol{u}_1^* = \hat{\boldsymbol{u}}_1 - \frac{1}{2}\mu_{12}\boldsymbol{a}_{12} \tag{38}$$

Fig. 2. Simulation results for two-robot deadlock. Simulation parameters shown in bottom right panel. Note at $t = t_1$, $D(t) = \beta_+^1(t)$ and $\mu_{12}(t)$ switches on, similarly at $t = t_2$, $\mu_{21}(t)$ switches on. Finally, $D(t) \longrightarrow D_s$.

Here $\mu_{12} \neq 0$ because the collision avoidance constraint of robot one has switched to active at t_1 *i.e.* $\boldsymbol{a}_{12}^T(t)\boldsymbol{u}_1^*(t) = b_{12}(t) \ \forall \ t \geq t_1$. We can compute μ_{12} as follows

$$\mu_{12} = 2\frac{\boldsymbol{a}_{12}^T\hat{\boldsymbol{u}}_1 - b_{12}}{\|\boldsymbol{a}_{12}\|^2} \tag{39}$$

Therefore, the dynamics of robot one $\forall t \geq t_1$ are

$$\dot{\boldsymbol{p}}_1 = \hat{\boldsymbol{u}}_1 - \frac{\boldsymbol{a}_{12}^T\hat{\boldsymbol{u}}_1 - b_{12}}{\|\boldsymbol{a}_{12}\|^2}\boldsymbol{a}_{12}$$

$$= \underbrace{\hat{\boldsymbol{u}}_1 - \frac{\boldsymbol{a}_{12}^T\hat{\boldsymbol{u}}_1}{\|\boldsymbol{a}_{12}\|^2}\boldsymbol{a}_{12}}_{\boldsymbol{u}_\perp} + \underbrace{\frac{b_{12}}{\|\boldsymbol{a}_{12}\|^2}\boldsymbol{a}_{12}}_{\boldsymbol{u}_\parallel} \tag{40}$$

On closer inspection, note that $\boldsymbol{u}_\perp \perp \boldsymbol{a}_{12} \iff \boldsymbol{u}_\perp \perp -\Delta\boldsymbol{p}_{12}$. It is difficult to analytically integrate (40). Instead, we will show via recursion that the position of robot one can be expressed as

$$\boldsymbol{p}_1(t) = \boldsymbol{p}_{d_1} - D_{G_1}\eta(t)\hat{\boldsymbol{e}}_\alpha \tag{41}$$

for some function $\eta(t) \ \forall \ t \geq t_1$. This expression is valid at $t = t_1$ for $\eta(t_1) = e^{-k_{p_1}t_1}$ as shown in (29). This representation highlights that the position of robot one is confined along $\hat{\boldsymbol{e}}_\alpha$. We will show that this property is maintained throughout phase 2 because the component of velocity input to robot one perpendicular to $\hat{\boldsymbol{e}}_\alpha$ will vanish (which will become the cause of *deadlock*). Recall at $t = t_1$

$$\boldsymbol{a}_{12}(t_1) = \Delta\boldsymbol{p}_{21}(t_1) = D(t_1)\hat{\boldsymbol{e}}_\alpha \tag{42}$$

Therefore, $\boldsymbol{u}_\perp(t_1) = \hat{\boldsymbol{u}}_1 - \frac{\boldsymbol{a}_{12}^T\hat{\boldsymbol{u}}_1}{\|\boldsymbol{a}_{12}\|^2}\boldsymbol{a}_{12}$

$$= k_{p_1}D_{G_1}\eta(t_1)\hat{\boldsymbol{e}}_\alpha$$

$$- \frac{D(t_1)\hat{\boldsymbol{e}}_\alpha^T\big(k_{p_1}D_{G_1}\eta(t_1)\hat{\boldsymbol{e}}_\alpha\big)}{D^2(t_1)}(D(t_1)\hat{\boldsymbol{e}}_\alpha)$$

$$= \boldsymbol{0}$$

$$\boldsymbol{u}_\parallel(t_1) = \frac{b_{12}}{\|\boldsymbol{a}_{12}\|^2}\boldsymbol{a}_{12}$$

$$= \gamma\frac{D^2(t_1) - D_s^2}{4D(t_1)}\hat{\boldsymbol{e}}_\alpha \tag{43}$$

Thus, integrating the velocity for a small time step gives

$$\boldsymbol{p}_1(t_1 + \Delta t) = \boldsymbol{p}_1(t_1) + \Delta t\big(\boldsymbol{u}_\perp(t_1) + \boldsymbol{u}_\parallel(t_1)\big)$$

$$= \boldsymbol{p}_{d_1} - D_{G_1}\bigg(\eta(t_1) - \Delta t\gamma\frac{D^2(t_1) - D_s^2}{4D_{G_1}D(t_1)}\bigg)\hat{\boldsymbol{e}}_\alpha$$

$$= \boldsymbol{p}_{d_1} - D_{G_1}\eta(t_1 + \Delta t)\hat{\boldsymbol{e}}_\alpha \tag{44}$$

Through (44), we have demonstrated that the updated position of robot one admits the general form given by (41). This is because the perpendicular component of the velocity vanishes if the robot is situated on the line segment connecting its goals. As a result, the robot never acquires any displacement along the perpendicular component. Hence, the dynamics of robot one are always

$$\dot{\boldsymbol{p}}_1 = \boldsymbol{u}_\parallel = \gamma\frac{\|\Delta\boldsymbol{p}_{21}\|^2 - D_s^2}{4\|\Delta\boldsymbol{p}_{21}\|^2}\Delta\boldsymbol{p}_{21}, \tag{45}$$

$\forall t \geq t_1$. The relative dynamics are

$$\dot{\Delta\boldsymbol{p}_{21}} = -\gamma\frac{\|\Delta\boldsymbol{p}_{21}\|^2 - D_s^2}{4\|\Delta\boldsymbol{p}_{21}\|^2}\Delta\boldsymbol{p}_{21} - k_{p_2}(\boldsymbol{p_2} - \boldsymbol{p}_{d_2}) \tag{46}$$

Let $\Delta\boldsymbol{p}_{21}(t) = D(t)\hat{\boldsymbol{e}}_\alpha$, then we get for $t \geq t_1$

$$\dot{D}(t) = -\gamma\frac{D^2(t) - D_s^2}{4D(t)} - k_{p_2}D_{G_2}e^{-k_{p_2}t} \tag{47}$$

where $D(t_1) = \beta_+^1(t_1) > D_s$. Note that for $D(t) > D_s$, $\dot{D}(t) < 0 \implies D(t)$ is monotonically decreasing at least until t_c where $t_c := \{t|D(t) = D_s\}$. Recall from phase 1 that the collision avoidance constraint of robot two is inactive *i.e.* $f_{21}(\hat{\boldsymbol{u}}_2(t)) < 0$ as long as $D(t) > \beta_+^2(t)$. Additionally, recall that $\beta_+^2(t)$ is monotonically decreasing with respect to time and converges to D_s. Moreover, from phase 1, recall that $D(t_1) = \beta_+^1(t_1) > \beta_+^2(t_1)$. Hence, there exists a time $t_2 \leq t_c$ at which $D(t) = \beta_+^2(t)$. This time t_2 is precisely the time in def. (36). See Fig. (2) for an illustration of phase 2 which ends at $t = t_2$ when $D(t) = \beta_+^2(t)$. Using the approach in **Lemma 3**, the distance between robots monotonically decreases $\forall t \in [t_1, t_2)$. This concludes phase 2 and marks the start of phase 3. $\blacksquare$

4.3 Phase 3

In phase three, the collision avoidance constraints of both robots become active *i.e.* $\boldsymbol{a}_{12}^T\boldsymbol{u}_1^* = b_{12}$ and $\boldsymbol{a}_{21}^T\boldsymbol{u}_2^* = b_{21}$. Therefore, the controls on the robots are

$$\boldsymbol{u}_1^* = \hat{\boldsymbol{u}}_1 - \frac{1}{2}\mu_{12}\boldsymbol{a}_{12} \ , \ \boldsymbol{u}_2^* = \hat{\boldsymbol{u}}_2 - \frac{1}{2}\mu_{21}\boldsymbol{a}_{21} \tag{48}$$

where, $\mu_{12} = 2\frac{\boldsymbol{a}_{12}^T\hat{\boldsymbol{u}}_1 - b_{12}}{\|\boldsymbol{a}_{12}\|^2} \ , \ \mu_{21} = 2\frac{\boldsymbol{a}_{21}^T\hat{\boldsymbol{u}}_2 - b_{21}}{\|\boldsymbol{a}_{21}\|^2} \tag{49}$

Following the approach in phase 2, we can show that the components of velocities in $\boldsymbol{u}_i^*$ perpendicular to $\hat{\boldsymbol{e}}_\alpha$ vanish. Therefore, the resulting dynamics of the robots are:

$$\dot{\boldsymbol{p}}_1 = +\gamma\frac{\|\Delta\boldsymbol{p}_{21}\|^2 - D_s^2}{4\|\Delta\boldsymbol{p}_{21}\|^2}\Delta\boldsymbol{p}_{21}$$

$$\dot{\boldsymbol{p}}_2 = -\gamma\frac{\|\Delta\boldsymbol{p}_{21}\|^2 - D_s^2}{4\|\Delta\boldsymbol{p}_{21}\|^2}\Delta\boldsymbol{p}_{21} \tag{50}$$

$$\implies \dot{\Delta\boldsymbol{p}_{21}} = -\gamma\frac{\|\Delta\boldsymbol{p}_{21}\|^2 - D_s^2}{2\|\Delta\boldsymbol{p}_{21}\|^2}\Delta\boldsymbol{p}_{21} \tag{51}$$

Lemma 5. *The distance between robots converges to the safety margin D_s at which point they stop moving*

Proof. Letting $\Delta\boldsymbol{p}_{21}(t) = D(t)\hat{\boldsymbol{e}}_\alpha$ in (51)

$$\dot{D}(t) = -\gamma \frac{D^2(t) - D_s^2}{2D(t)} \qquad (52)$$

where $D(t_2) = \beta_+^2(t_2) > D_s$. The solution to this is

$$D(t) = \sqrt{(D^2(t_2) - D_s^2)e^{-\gamma(t-t_2)} + D_s^2} \qquad (53)$$

Therefore $D(t) \longrightarrow D_s$ and likewise, $\|\Delta \boldsymbol{p}_{12}(t)\| \longrightarrow D_s$. Therefore, the robots will be just at the verge of colliding. Moreover, note from (50) that as $\|\Delta \boldsymbol{p}_{12}(t)\| \longrightarrow D_s$, $\dot{\boldsymbol{p}}_1 \longrightarrow \boldsymbol{0}$, $\dot{\boldsymbol{p}}_2 \longrightarrow \boldsymbol{0}$, *i.e.* the robots stop moving. ∎

Proof of Theorem 1: From **Lemma 3** and **Lemma 4**, it follows that phase 1 and phase 2 culminate in a finite time, so the robots enter phase 3. In phase 3, **Lemma 5** shows that the robots eventually stop moving. However, once they stop, note that $\lim_{t \longrightarrow \infty} \Delta \boldsymbol{p}_{21}(t) = D_s \hat{\boldsymbol{e}}_\alpha$, yet $\Delta \boldsymbol{p}_{d_{21}} = -(D_{G_1} + D_{G_2} - D_{init.})\hat{\boldsymbol{e}}_\alpha$. Therefore, the robots are not at their goals (because the goal vector is anti-parallel to the vector connecting the robots). Hence, we conclude that the robots have fallen in *deadlock* ∎

Takeaway: We have demonstrated that two robots fall in deadlock given initial conditions (17) and goals (18). This is because the *geometric arrangement of initial positions and goals prevents both $\hat{\boldsymbol{u}}$ and the QP to output velocities perpendicular to the $\hat{\boldsymbol{e}}_\alpha$ direction.* In phase 1, the prescribed controllers were only along $\hat{\boldsymbol{e}}_\alpha$ as noted in (32), thus $\boldsymbol{u}_\perp = \boldsymbol{0}$. In phase 2, we explicitly calculated $\boldsymbol{u}_\perp = \boldsymbol{0}$ in (43). In Phase 3, same arguments applied. Thus, with the control always along $\boldsymbol{u}_\parallel \parallel \hat{\boldsymbol{e}}_\alpha$, the only way to reach the goals would involve intersection of the robots *i.e.* collisions. This is why, the QP based controller decides to prevent collisions from happening by forcing the robots to stall, resulting in deadlock.

5. THREE-ROBOT DEADLOCK

We demonstrate another scenario prone to deadlock, which consists of three robots positioned on the vertices of an equilateral triangle, and required to stabilize to their respective antipodal positions. For simplicity, we assume that all prescribed controller gains are *identical*, as are the distances of the robots' initial positions to their goals. Let $\boldsymbol{p}_i(t) \in \mathbb{R}^2$ be the position of robot $i \in \{1, 2, 3\}$ given as

$$\boldsymbol{p}_1(0) = (x_0, y_0)$$
$$\boldsymbol{p}_2(0) = \boldsymbol{p}_1(0) + D_{init}\hat{\boldsymbol{e}}_\alpha$$
$$\boldsymbol{p}_3(0) = \boldsymbol{p}_2(0) + D_{init}\hat{\boldsymbol{e}}_{\alpha + \frac{2\pi}{3}} \qquad (54)$$

Assume that the goal of each robot is diametrically opposite to its initial position *i.e.*

$$\boldsymbol{p}_{d_i} = \boldsymbol{p}_i(0) + \frac{\sqrt{3}D_G}{D_{init.}}(\boldsymbol{c} - \boldsymbol{p}_i(0)) \qquad (55)$$

for $i \in \{1, 2, 3\}$ where $\boldsymbol{c} = \frac{1}{3}\sum_{i=1}^3 \boldsymbol{p}_i(0)$ is the centroid of the equilateral triangle formed by the initial positions and D_G is the distance of each robot from it's goal. Note here that the positions of the robots and their goals are *not collinear* as was assumed in the two-robot case. Nevertheless, this scenario is still prone to deadlock, because of (1) the geometric symmetry in the initial positions of robots and goals and (2) identical controller gains.

Assumption 2. $\sqrt{3}D_G > D_{init.}$

We will use this assumption in **Lemma 9** to establish the inevitability of deadlock. We now formally state the deadlock incidence result as follows.

Theorem 6. *Given the initial positions of robots as in (54) and desired goals as in (55), the controls generated by (7) will cause the robots to fall in deadlock.*

Our proof will heavily draw upon the ideas from deadlock in the two robot case. The overall sketch is as follows:

(1) First, we analyze the controls returned by the QP at $t = 0$. We show in **Lemma 7** that if the initial distance between robots is greater than a certain critical distance, then at $t = 0$, the collision avoidance constraints of all robots are inactive, therefore $\boldsymbol{u}_i^*(0) = \hat{\boldsymbol{u}}_i(0) \ \forall i \in \{1, 2, 3\}$.
(2) Next, we show that the future motion of robots can be broken into two successive phases. In phase 1, the collision avoidance constraints of all robots stay inactive, so they use $\hat{\boldsymbol{u}}_i(t) \ \forall i \in \{1, 2, 3\}$. We prove in **Lemma 8** that using $\hat{\boldsymbol{u}}(t)$, the robots move on the vertices of an equilateral triangle. Next, in **Lemma 9**, we demonstrate that there exists a finite time when phase 1 culminates. More importantly, this time is identical for all robots because of the symmetry that follows from **Lemma 8**
(3) Next, phase 2 begins during which all constraints are active. We show in **Lemma 10** that the distance between robots converges to D_s, their velocities converge to zero while the robots are still away from their goals, thus establishing *deadlock.*

Recall from (16) that the control for robot i is

$$\boldsymbol{u}_i^* = \hat{\boldsymbol{u}}_i - \frac{1}{2} \sum_{j \in \{1, 2, 3\} \backslash i} \mu_{ij} \boldsymbol{a}_{ij} \qquad (56)$$

Here, the value of μ_{ij} depends on whether the collision avoidance constraint $\boldsymbol{a}_{ij}^T \boldsymbol{u}_i \leq b_{ij}$ is active or inactive at $\boldsymbol{u}_i = \boldsymbol{u}_i^*$. Therefore, we will focus on the flag $f_{ij}(\boldsymbol{u}_i) = \boldsymbol{a}_{ij}^T \boldsymbol{u}_i - b_{ij}$ to decide the control for robot i. We begin our analysis at $t = 0$ and show in the next lemma that if the initial distance between the robots is greater than the critical distance, then at $t = 0$, both robots have inactive constraints. We define critical distance as follows:

$$\beta_+ = \frac{\sqrt{3}D_G k_p}{\gamma} + \sqrt{\frac{3D_G^2 k_p^2}{\gamma^2} + D_s^2} \qquad (57)$$

Lemma 7. *If $D_{init.} > \beta_+$, then $\boldsymbol{u}_i^*(0) = \hat{\boldsymbol{u}}_i(0) \ \forall i$*

Proof. To keep calculations brief, we compute the flag $f_{ij}(\hat{\boldsymbol{u}}_i(0))$ for $i = 1$, $j = 2$. Using (54)-(55), we have

$$f_{12}(\hat{\boldsymbol{u}}_1(0))) = \boldsymbol{a}_{12}^T(0)\hat{\boldsymbol{u}}_1(0) - b_{12}(0)$$

$$= -\frac{\gamma}{4}D_{init}^2 + \frac{\sqrt{3}D_G k_p}{2}D_{init} + \frac{\gamma}{4}D_s^2$$

$$:= g(D_{init.}) \qquad (58)$$

We can show that $f_{ij}(\hat{\boldsymbol{u}}_i) = g(D_{init.}) \ \forall i \in \{1, 2, 3\}, j \neq i$ because of the equilateral configuration at $t = 0$. $g(D_{init.})$ is a quadratic polynomial in $D_{init.}$ with a zero at β_+ ((57)). Therefore, $D_{init} \in (\beta_+, \infty) \implies g(D_{init.}) < 0 \iff f_{ij}(\hat{\boldsymbol{u}}_i(0)) < 0 \ \forall i \in \{1, 2, 3\}, \forall j \in \{1, 2, 3\} \backslash i, \iff \boldsymbol{u}_i^*(0) = \hat{\boldsymbol{u}}_i(0) \ \forall i \in \{1, 2, 3\}$ ∎

Assumption 3. *WLOG assume at $t = 0$, $D_{init.} > \beta_+$.*

From assumption (3) and Lemma 7, it follows that at $t = 0$, **all** collision avoidance constraints of **all** robots are inactive. Therefore, it is safe to assume that these constraints also remain inactive for a finite duration after $t = 0$, which is precisely phase 1 as discussed before.

5.1 Phase 1

Assume that all robots continue to follow their prescribed controls until time t_1. Hence their positions are:

$$\boldsymbol{p}_i(t) = (\boldsymbol{p}_i(0) - \boldsymbol{p}_{d_i})e^{-k_p t} + \boldsymbol{p}_{d_i} \quad \forall t \in [0, t_1] \qquad (59)$$

Next we show that these positions evolve along the vertices of an equilateral triangle.

Lemma 8. *All robots continue to move in an equilateral triangular configuration with centroid at $\boldsymbol{c}(0)$*

Proof. Using (59), the centroid's position is given by

$$\boldsymbol{c}(t) = \frac{1}{3}\sum_{i=1}^{3}\boldsymbol{p}_i(t)$$

$$= \underbrace{\frac{1}{3}\sum_{i=1}^{3}(\boldsymbol{p}_i(0) - \boldsymbol{p}_{d_i})e^{-k_p t}}_{\boldsymbol{0}} + \underbrace{\frac{1}{3}\sum_{i=1}^{3}\boldsymbol{p}_{d_i}}_{\boldsymbol{c}(0)}$$

$$= \boldsymbol{c}(0) \qquad (60)$$

The distance between robot i and robot j is given by

$$\|\Delta\boldsymbol{p}_{ij}(t)\| = \sqrt{\underbrace{\|\Delta\boldsymbol{p}_{ij}(0)\|^2}_{\text{term 1}} e^{-2k_p t} + \underbrace{\|\Delta\boldsymbol{p}_{d_{ij}}\|^2}_{\text{term 2}}(1 - e^{-k_p t})^2 +}$$
$$\underbrace{2\,\Delta\boldsymbol{p}_{ij}^T(0)\Delta\boldsymbol{p}_{d_{ij}}(e^{-k_p t} - e^{-2k_p t})}_{\text{term 3}} \qquad (61)$$

One can show that term 1, term 2 and term 3 are identical for all $i, j \in \{1, 2, 3\}, j \neq i$ using (54), (55). Therefore, the distance of robot i from robot $j \neq i$ is same for all $i \in \{1, 2, 3\}$, hence the robots move along the vertices of an equilateral triangle. A second invariant is the angle made by the vector connecting robots i, j with the X_w axis of the world. This can be shown by demonstrating that $\Delta\boldsymbol{p}_{ij}(t)$ remains parallel to $\Delta\boldsymbol{p}_{ij}(0)$ as follows

$$\Delta\boldsymbol{p}_{ij}(t) \times \Delta\boldsymbol{p}_{ij}(0) = \underbrace{\big(\Delta\boldsymbol{p}_{ij}(0) \times \Delta\boldsymbol{p}_{ij}(0)\big)}_{\boldsymbol{0}}e^{-k_p t}$$
$$+ \underbrace{\big(\Delta\boldsymbol{p}_{d_{ij}} \times \Delta\boldsymbol{p}_{ij}(0)\big)}_{\text{term 1}}(1 - e^{-k_p t})$$
$$= \boldsymbol{0} \qquad (62)$$

Term 1 vanishes because $\Delta\boldsymbol{p}_{d_{ij}}$ is anti-parallel to $\Delta\boldsymbol{p}_{ij}(0)$ using (54), (55) Thus, the positions of the robots can still be written in the form similar to (54)

$$\boldsymbol{p}_1(t) = e^{-k_p t}\boldsymbol{p}_1(0) + (1 - e^{-k_p t})\boldsymbol{p}_{d_1}$$
$$\boldsymbol{p}_2(t) = \boldsymbol{p}_1(t) + \tilde{D}(t)\hat{\boldsymbol{e}}_\alpha$$
$$\boldsymbol{p}_3(t) = \boldsymbol{p}_2(t) + \tilde{D}(t)\hat{\boldsymbol{e}}_{\alpha+\frac{2\pi}{3}} \qquad (63)$$

where $\tilde{D}(0) = D_{init.}$. Here, the angle between $\Delta\boldsymbol{p}_{21}$ and X_w is still α as in (54) because of (62). Thus, the robots move along the vertices of an equliateral triangle using $\hat{\boldsymbol{u}}_i(t) \,\forall i \in \{1, 2, 3\}$. *This symmetry is because (1) $\hat{\boldsymbol{u}}_i(t)$ has identical gains (i.e. k_p) $\forall i$ and (2) the distance of initial position to goal is identical for all robots (D_G)* ∎

Note that in (63), we can compute $\tilde{D}(t)$ as follows:

$$\tilde{D}(t) = \hat{\boldsymbol{e}}_\alpha^T \Delta\boldsymbol{p}_{21}(t)$$
$$= \hat{\boldsymbol{e}}_\alpha^T \left(\Delta\boldsymbol{p}_{21}(0)e^{-k_p t} + \Delta\boldsymbol{p}_{d_{21}}(1 - e^{-k_p t}) \right)$$
$$= (D_{init.} - \sqrt{3}D_G) + \sqrt{3}D_G e^{-k_p t} \qquad (64)$$

Using this definition of $\tilde{D}(t)$, we now demonstrate that there exists a time when all the collision avoidance constraints will inevitably become active.

Lemma 9. *There exists a time t_{ij} when $f_{ij}(\hat{\boldsymbol{u}}_i(t)) = \boldsymbol{a}_{ij}^T(t)\hat{\boldsymbol{u}}_i(t) - b_{ij}(t) = 0$ i.e. when the collision avoidance constraint of robot i with robot j becomes active. Furthermore, t_{ij} is identical $\forall i \in \{1, 2, 3\}, j \in \{1, 2, 3\}\backslash i$*

Proof. Using (59), we can find that $f_{ij}(\hat{\boldsymbol{u}}_i(t))$ (as a function of time) is identical for $\forall i \in \{1, 2, 3\}$, $j \in \{1, 2, 3\}\backslash i$. This is again due to the symmetry in the positions at time t. Now, we evaluate $f_{ij}(\hat{\boldsymbol{u}}_i)$ as a function of $\tilde{D}$. For brevity, we evaluate this for $i = 1$, $j = 2$:

$$g(\tilde{D}) := f_{12}(\hat{\boldsymbol{u}}_1) = \boldsymbol{a}_{12}^T\hat{\boldsymbol{u}}_1 - b_{12}$$
$$= -\frac{\gamma}{4}\tilde{D}^2(t) + \frac{\sqrt{3}}{2}k_p D_G e^{-k_p t}\tilde{D}(t) + \frac{\gamma}{4}D_s^2 \qquad (65)$$

Note that $g(\tilde{D})$ is quadratic in $\tilde{D}$ with a zero at

$$\beta_+(t) = \frac{\sqrt{3}D_G k_p e^{-k_p t}}{\gamma} + \sqrt{\left(\frac{\sqrt{3}D_G k_p e^{-k_p t}}{\gamma}\right)^2 + D_s^2}$$

Therefore, if $\tilde{D}(t) \leq \beta_+(t) \implies f_{12}(\hat{\boldsymbol{u}}_1(t)) \geq 0$. Now, note from (64) that $\tilde{D}(t)$ is monotonically decreasing with t, $\tilde{D}(0) = D_{init.} > \beta_+$ (from Assumption (3)). Also, note that $\lim_{t\to\infty}\tilde{D}(t) = D_{init.} - \sqrt{3}D_G < 0$ from Assumption (2). Similarly, $\beta_+(t)$ is monotonically decreasing. $\beta_+(0) < D_{init.}$ and $\lim_{t\to\infty}\beta_+(t) = D_s > 0$. Therefore, there exists a time when $\tilde{D}(t)$ intersects $\beta_+(t)$ i.e. $t_1 = \{t|\tilde{D}(t) = \beta_+(t)\}$. This is equivalent to $t_1 = \{t|f_{ij}(\hat{\boldsymbol{u}}_i(t)) = 0 \,\forall i \in \{1, 2, 3\}, j \in \{1, 2, 3\}\backslash i\}$. This is precisely when constraints of **all** robots become active. ∎

5.2 Phase 2

Following $t \geq t_1$, the collision avoidance constraints of all robots become active. Thus, the control on each robot is

$$\boldsymbol{u}_i^* = \hat{\boldsymbol{u}}_i - \frac{1}{2}\sum_{j\in\{1,2,3\}\backslash i}\mu_{ij}\boldsymbol{a}_{ij} \qquad (66)$$

where now, $\mu_{ij} \neq 0 \,\forall i \in \{1, 2, 3\}, \forall j \in \{1, 2, 3\}\backslash i$. For e.g., for robot one, collision avoidance constraints with both robots two and three become active. Therefore, using $\boldsymbol{a}_{12}^T\boldsymbol{u}_1^* = b_{12}$ and $\boldsymbol{a}_{13}^T\boldsymbol{u}_1^* = b_{13}$, we can obtain μ_{12} and μ_{13} analytically, which will give the control $\boldsymbol{u}_1^*$. Following the arguments in phase 3 for the two robot case, we can incrementally compute the controls by solving for Lagrange multipliers at t_1, applying the control $\boldsymbol{u}_i^*(t_1)$ and updating positions and so on for all future time. We can demonstrate that the positions of the robots can still be written as

$$\boldsymbol{p}_1(t) = \eta(t)\boldsymbol{p}_1(0) + (1 - \eta(t))\boldsymbol{p}_{d_1}$$
$$\boldsymbol{p}_2(t) = \boldsymbol{p}_1(t) + D(t)\hat{\boldsymbol{e}}_\alpha$$
$$\boldsymbol{p}_3(t) = \boldsymbol{p}_2(t) + D(t)\hat{\boldsymbol{e}}_{\alpha+\frac{2\pi}{3}} \qquad (67)$$

for $t \geq t_1$ for some function $\eta(t)$ with $\eta(t_1) = e^{-k_p t_1}$. Following arguments as in phase 3 of the two robot deadlock, dynamics of robot $i \in \{1, 2, 3\}$ are:

$$\dot{\boldsymbol{p}}_i = \sqrt{3}\gamma \frac{D^2(t) - D_s^2}{6D(t)} \hat{\boldsymbol{e}}_{\alpha + (4i-3)\frac{\pi}{6}} \qquad (68)$$

$$\implies \dot{\Delta \boldsymbol{p}}_{12} = \gamma \frac{D^2(t) - D_s^2}{2D(t)} \hat{\boldsymbol{e}}_\alpha \qquad (69)$$

Lemma 10. *The distance between the robots converges to the safety margin D_s and the robots stop moving*

Proof. Noting From (67) that $\Delta \boldsymbol{p}_{12}(t) = -D(t)\hat{\boldsymbol{e}}_\alpha$ and combining with (69), we deduce that

$$\dot{D}(t) = -\gamma \frac{D^2(t) - D_s^2}{2D(t)} \qquad \forall t \geq t_1$$

$$\implies D(t) = \sqrt{(D^2(t_1) - D_s^2)e^{-\gamma(t-t_1)} + D_s^2}$$

$$\implies \lim_{t \to \infty} D(t) = D_s \qquad (70)$$

Hence, it follows from (68) that $\dot{\boldsymbol{p}}_i \longrightarrow \boldsymbol{0} \; \forall i \in \{1, 2, 3\}$ ∎

Proof of Theorem 6: From **Lemma 9**, it follows that the robots enter phase 2 at $t = t_1$. Once in phase 2, from **Lemma 10** it follows that the robots eventually stop moving. Additionally, note that $\lim_{t \to \infty} \Delta \boldsymbol{p}_{12}(t) = -D_s \hat{\boldsymbol{e}}_\alpha$ yet $\Delta \boldsymbol{p}_{d_{12}} = (\sqrt{3}D_G - D_{init.})\hat{\boldsymbol{e}}_\alpha \neq -D_s \hat{\boldsymbol{e}}_\alpha$ (from (55) and Assumption 2). Therefore, the robots are not at their goals, and static, thus they have fallen in *deadlock*. ∎

Takeaway: Deadlock happens here because each robot's velocity is always pointing towards its goal and not perpendicular to it. In phase 1, this velocity is along $\hat{\boldsymbol{u}}$ (which by definition is towards the goal). Likewise, we can show that the same holds true in phase 2. Additionally, all robots have identical speed at a given time as well. Hence, collisions would be inevitable at the centroid. Therefore, CBF-QPs cause the robots to stall which results in deadlock.

6. CONCLUSIONS

In this paper, we analyzed CBFs for synthesizing safe controllers for multirobot systems, that also help perform a given task such as goal stabilization. We handpicked a combination of initial conditions and goals to show how they fail to reach their goals in the interest of maintaining safety. The key takeaway from the two examples we considered, is that geometric symmetry constrains CBFs to generate velocities in directions that render deadlock stable. For example, for the two robot case, a velocity along $\hat{\boldsymbol{e}}_{\alpha + \frac{\pi}{2}}$ could have resolved deadlock easily but neither $\hat{\boldsymbol{u}}$ nor CBFs identify such inputs, likewise in the three-robot case. Our simulations reveal that deadlocks can also happen in large N and asymmetric cases, for example, when goals are not antipodal. Therefore, in future work, we will consider general analysis for symmetric and asymmetric N robot systems to reveal general scenarios prone to deadlock. Secondly, we relied on duality theory to aid with this analysis. Our approach using KKT conditions is general and can be extended to any optimization based reactive control synthesis method. In future, we will extend this tool to algorithms such as velocity obstacles. Finally, we will consider different dynamics models such as double-integrator and nonholonomic type.

REFERENCES

Ames, A.D., Xu, X., Grizzle, J.W., and Tabuada, P. (2017). Control barrier function based quadratic programs for safety critical systems. IEEE Transactions on Automatic Control, 62(8), 3861–3876.

Borrmann, U., Wang, L., Ames, A.D., and Egerstedt, M. (2015). Control barrier certificates for safe swarm behavior. IFAC-PapersOnLine, 48(27), 68–73.

Boyd, S. and Vandenberghe, L. (2004). Convex optimization. Cambridge university press.

Burgard, W., Moors, M., Stachniss, C., and Schneider, F.E. (2005). Coordinated multi-robot exploration. IEEE Transactions on robotics, 21(3), 376–386.

Cortes, J., Martinez, S., Karatas, T., and Bullo, F. (2004). Coverage control for mobile sensing networks. IEEE Transactions on robotics and Automation, 20(2), 243–255.

Jager, M. and Nebel, B. (????). Decentralized collision avoidance, deadlock detection, and deadlock resolution for multiple mobile robots. In Proceedings 2001 IEEE/RSJ International Conference on Intelligent Robots and Systems. Expanding the Societal Role of Robotics in the the Next Millennium (Cat. No. 01CH37180), volume 3, 1213–1219. IEEE.

Kantor, G., Singh, S., Peterson, R., Rus, D., Das, A., Kumar, V., Pereira, G., and Spletzer, J. (2003). Distributed search and rescue with robot and sensor teams. In Field and Service Robotics, 529–538. Springer.

Li, Y., Gupta, K., and Payandeh, S. (2005). Motion planning of multiple agents in virtual environments using coordination graphs. In Proceedings of the 2005 IEEE International Conference on Robotics and Automation, 378–383. IEEE.

O'Donnell, P. (1989). Deadlockfree and collision-free coordination of two robot manipulators. In Proc. IEEE International Conference on Robotics and Automation, 484–489.

Olfati-Saber, R., Fax, J.A., and Murray, R.M. (2007). Consensus and cooperation in networked multi-agent systems. Proceedings of the IEEE, 95(1), 215–233.

Petti, S. and Fraichard, T. (2005). Safe motion planning in dynamic environments. In 2005 IEEE/RSJ International Conference on Intelligent Robots and Systems, 2210–2215. IEEE.

Rodríguez-Seda, E.J., Stipanović, D.M., and Spong, M.W. (2016). Guaranteed collision avoidance for autonomous systems with acceleration constraints and sensing uncertainties. Journal of Optimization Theory and Applications, 168(3), 1014–1038.

Wang, L., Ames, A.D., and Egerstedt, M. (2017). Safety barrier certificates for collisions-free multirobot systems. IEEE Transactions on Robotics, 33(3), 661–674.

Wei, T. and Liu, C. (2019). Safe control algorithms using energy functions: A unified framework, benchmark, and new directions. arXiv:1908.01883.

Yamaguchi, H. (1999). A cooperative hunting behavior by mobile-robot troops. the International Journal of robotics Research, 18(9), 931–940.